Article

QbD-Assisted Development and Optimization of Doxycycline Hyclate- and Hydroxyapatite-Loaded Nanoparticles for Periodontal Delivery

Pooja Jain, Mohd. Aamir Mirza, Enam Reyaz, Mirza Adil Beg, Angamuthu Selvapandiyan, Nazeer Hasan, Akbar Naqvi, Naseef Punnoth Poonkuzhi, Mohammad Saheer Kuruniyan, Harlokesh Narayan Yadav, Farhan J. Ahmad, and Zeenat Iqbal*
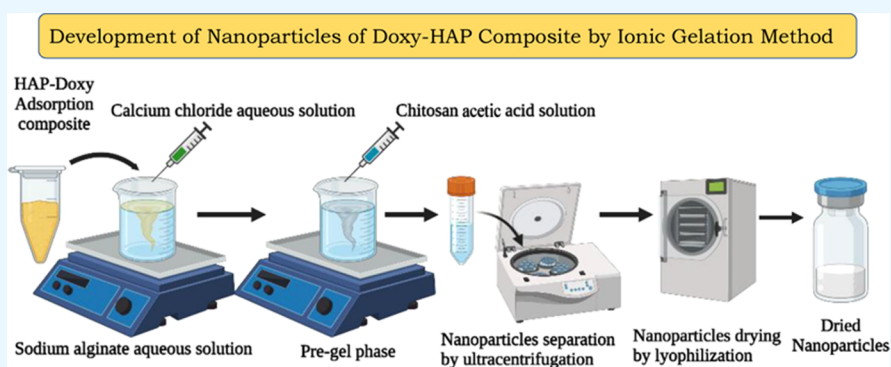
Read Online

ACCESS | Metrics & More | Article Recommendations

Development of Nanoparticles of Doxy-HAP Composite by Ionic Gelation Method

ABSTRACT: The current research aims to develop a carrier system for the delivery of a matrix metalloproteinase (MMP) inhibitor along with a bioceramic agent to the periodontal pocket. It is proposed that the present system, if given along with a systemic antibiotic, would be a fruitful approach for periodontitis amelioration. To fulfill the aforementioned objective, a doxycycline hyclate- and hydroxyapatite-adsorbed composite was prepared by a physical adsorption method and successfully loaded inside sodium alginate−chitosan nanoparticles and optimized based on particle size and drug content. Optimized formulation was then subjected to different evaluation parameters like encapsulation efficiency, hydroxyapatite content, ζ potential, surface morphology, in vitro drug release, cell line studies, and stability studies. For the optimized formulation, particle size, polydispersity index (PDI), entrapment efficiency, ζ potential, and drug content were found to be 336.50 nm, 0.23, 41.77%, −13.85 mV, and 14.00%, respectively. The surface morphology of the placebo and adsorbed composite-loaded nanoparticles as observed by scanning electron microscopy (SEM) and transmission electron microscopy (TEM) revealed the spherical shape and rough surface of the particles. In gingival crevicular fluid (GCF) 7.6, a sustained drug release profile was obtained up to 36 h. In vitro % viability studies performed on murine fibroblast cells (NIH3T3) and human periodontal ligament (hPDL) cell lines confirmed the proliferative nature of the formulation. Also, when subjected to stability studies for 4 weeks, particle size, PDI, and drug content did not vary considerably, thereby ensuring the stable nature of nanoparticles. Henceforth, sodium alginate−chitosan nanoparticles appeared to be a good carrier system for doxycycline hyclate and hydroxyapatite for periodontal therapy. If given along with a system antibiotic, the system will serve as a fruitful tool for infection-mediated periodontal regeneration and healing.

1. INTRODUCTION

Oral afflictions are a spectrum of globally prevalent diseases, and among these, periodontitis is the most prevalent with a global presence of 11.2%.[1] Periodontitis is an infection-mediated inflammation of gingiva and periodontium, leading to gingivitis, pyorrhea, and halitosis, wherein advanced stages result in the destruction of bone-supporting tissue, alveolar bone loss, and the development of periodontal pockets due to collagen destruction.[2,3] Recent studies suggested that periodontitis, 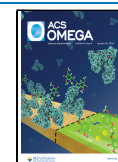by means of altering the inflammatory status for a number of systemic diseases, may eventually influence COVID-19 outcomes in an indirect manner.[4,5]
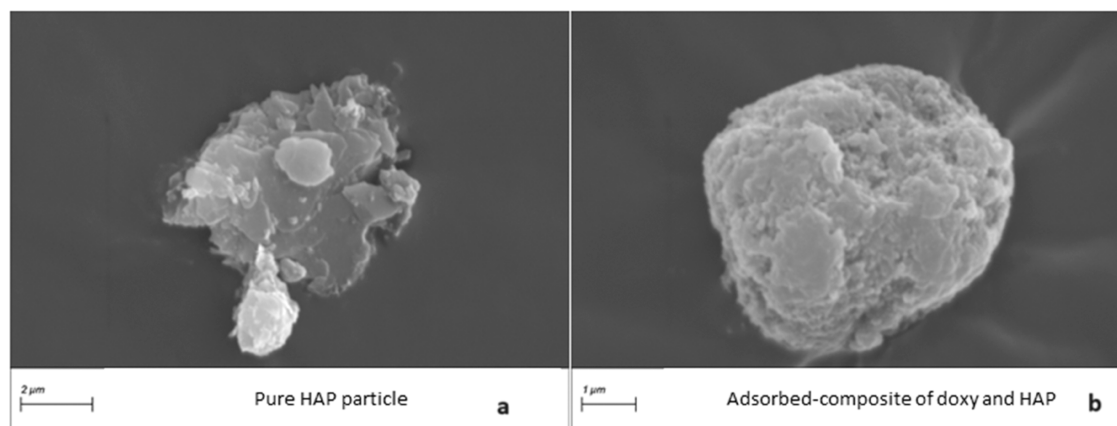
Figure 1. Morphology of HAP (a) and adsorbed composite of doxy and HAP (b).

Disease pathophysiology indicates that the vicious circle starts with biofilm deposition on the tooth surface, which then leads to host modulation in terms of inflammation, alveolar bone resorption, and, ultimately, edentulism. A common treatment strategy involves root planning, scaling, flap surgery, and periodontal pocket reduction surgery, along with systemic antibiotics and anti-inflammatory agents.[6−8] However, in all of the above-mentioned procedures, the diseased gingiva and alveolar bone are usually left for self-healing. But as the periodontal pockets are 2−10 mm in depth, it takes time to heal, which paves the way for further biofilm development and infection.[3]

Therefore, it is necessary that, along with antibiotics and anti-inflammatory drug therapy, a suitable system should be locally applied inside the periodontal pocket, which can support the healing of the gingiva and alveolar bone. Recently, the World Health Organization has approved the drug doxycycline hyclate (doxy) as MMP-8 (matrix metalloproteinase-8) and 13 inhibitors.[9,10] Doxy, when given in a subantimicrobial dose, can inhibit the collagen destruction of the gingiva.[11] A well-known bioceramic, namely, hydroxyapatite (HAP), is a natural osteo-inductor, is porous and granular in nature, and helps osteoblast cells by promoting alveolar bone desorption.[1] Henceforth, if HAP is combined with doxy, then the system may provide a speedy recovery of the tooth collagen and alveolar bone. The same hypothesis has been validated by in silico studies based on molecular docking.[12] Another approach adopted to have better therapeutic potential is the exploration of nanotechnology.[13,14] Nanoparticles have some advantages such as larger surface areas and higher penetrability than other granular bone repair materials. Nanoparticles with a uniform morphology also ensure improved site-specific or localized delivery.[15−18] Also, the literature suggests that the combination of doxy and HAP attenuates the progression of peri-implantitis.[19] Andrei et al. assessed the immunomodulatory effect of nano-HAP and doxycycline-loaded nanofibers in an animal model and reported effective improvements in clinical parameters.[20] Doxy-containing HAP scaffolds have been developed and explored as well for bone regeneration, and promising results have been obtained.[21] This prior art serves as the basis of the present work hypothesis. Therefore, in the present research, dual drug-loaded polymeric nanoparticles of doxy (doxycycline) and HAP (hydroxyapatite) have been prepared. Sodium alginate being a natural linear polysaccharide has wide applications in the food industry and bone tissue engineering and is also used as a vehicle in drug delivery systems.

When cross-linked with calcium chloride, it forms a pregel phase and finally forms nanoparticles when mixed with chitosan by the ionic gelation process. Chitosan being a natural alkali polysaccharide has shown potential in bone tissue engineering and drug delivery due to its biodegradability and biocompatibility.[22,23] Altogether, nanoparticles of sodium alginate and chitosan serve as a biodegradable carrier for the delivery of doxy and HAP.[24]

The formulation was optimized through quality by the design approach (QbD), which involves initial risk assessment, method optimization, and ultimately validation of the resultant method.[25,26] The literature supports that in recent years, a QbD-based optimization process has been extensively explored by researchers.[27] Nonetheless, it is proposed that the present system, if given along with the systemic antibiotic, would be a fruitful approach for periodontitis amelioration. Therefore, the current work aims at the development, optimization, and characterization of doxy- and HAP-loaded sodium alginate−chitosan nanoparticles for periodontal delivery. In order to achieve the aim, objectives such as the development of the adsorbed composite, nanoparticle development, optimization by quality by the design approach, characterization in terms of particle size, PDI, drug content, surface morphology, drug release studies, and in vitro cell line studies were laid down, and experiments were conducted. Altogether, the present work is a scientific pursuit for periodontal bone regeneration.

2. RESULTS AND DISCUSSION

2.1. Development and Characterization of the HAP-Doxy-Adsorbed Composite.
The adsorbed composite of HAP and doxy was developed by a physical adsorption method in a 3:1 ratio and characterized by scanning electron microscopy. Figure 1 shows the comparison between the morphology of pure HAP and the composite, wherein the HAP surface appears smooth, and the composite surface appears rough due to the deposition of doxy particles on the HAP surface. Further, it was found that 87% of the drug adhered to the HAP surface.

2.2. Development and Optimization of HAP-Doxy-Adsorbed Composite-Loaded Nanoparticles.
Prior to formulation development, the determination of the quality target product profile (QTPP) of the final product is the first step. QTPP also explains the critical quality attributes (CQAs). These are the attributes that define the desired quality standards of the product. Also, it is necessary to decide the criticality reason and acceptable ranges of each quality attribute.[28] Thus,

based upon the initial experimentation and literature search, the QTPP of nanoparticles was established, and particle size, polydispersity index (PDI), and drug content were selected as CQAs, as shown in Table 1.

Table 1. Quality Attributes and Reason for Their Criticality

quality attribute (range of acceptance)	reason for criticality
particle size (≤400 nm)	easy penetration
PDI (≤0.3)	to ensure the uniformity of size
% drug content (100)	for maximum utilization of the employed drug

For formulation development, HAP-Doxy-adsorbed composite-loaded nanoparticles of sodium alginate and chitosan were prepared by the cation-induced controlled gelification method. Briefly, a weighed and optimized amount of the composite was added to sodium alginate aqueous solution, and to this solution, calcium chloride aqueous solution was added dropwise. This resulted in the pregel phase, and to this phase, an acidic solution of chitosan was added dropwise, which led to the development of nanoparticles.

For optimization of nanoparticles, an initial risk assessment was performed, wherein the effect of sodium alginate (SA) concentration, calcium chloride ($CaCl_2$) concentration, speed of stirring, time of stirring, SA/ chitosan ratio, and quantity of the composite on particle size and PDI were studied (Table 2).

Table 2. Formulation Trials for the Initial Risk Assessment

formulation code	parameter	particle size (nm)	PDI
	Sodium Alginate Conc.		
N1	0.08% w/v	525.60	0.6
N2	0.06% w/v	325.80	0.7
N3	0.03% w/v	280.50	0.2
	Calcium Chloride Conc.		
N4	18 mM	648.30	0.8
N5	36 mM	799.30	0.1
N6	12 mM	1732.00	0.5
	Time of Stirring		
N7	1 h	650.00	0.9
N8	2 h	255.00	0.2
N9	3 h	105.3.00	0.9
	Stirring Speed		
N10	1200 rpm	325.00	0.2
N11	800 rpm	730.00	0.5
	SA/chitosan Ratio		
N12	10:1	280.00	0.2
N13	2:1	317.00	0.8
	Amount of the Complex		
N14	2 mg	200.00	0.2
N15	3 mg	250.00	0.3

It was observed that at high concentrations of sodium alginate, large size particles were formed. Also, at a 12 mM concentration of calcium chloride, a very large particle size was obtained. This might be because the interaction of sodium alginate and calcium chloride was not appropriate at these concentrations. It was observed that the high time of stirring and speed of stirring also affected the particle size and PDI. Another important factor, i.e., sodium alginate/chitosan ratio, was assessed at two levels, i.e., 10:1 and 2:1, and it was observed that a large particle size was obtained at the 2:1 ratio. This can be attributed to the fact that at

the 10:1 ratio, the functional groups of the pregel phase and chitosan solution were in stoichiometry for interaction, which gave rise to smaller size particles and high PDI. Moreover, when the effect of the quantity of the composite was assessed on particle size and PDI, no major difference was observed. Based on this, process variables such as stirring speed (1200 rpm), time of stirring (3 h), and material attributes such as SA/chitosan ratio (10:1) and amount of the composite (3 mg) were fixed, as shown in Table 3. The remaining two variables, i.e., sodium

Table 3. Optimized Values of Fixed Parameters for the Formulation

parameter	optimized value
time of stirring	3 h
stirring speed	1200 rpm
SA/chitosan ratio	10:1
amount of the complex	3 mg

alginate (0.03−0.06%w/v) and calcium chloride concentrations (18−36 mM), were treated as independent variables in the central composite design, and their effect on particle size and % drug content (dependent variables) was studied via 2^2 level factorial design. Table 4 shows the various design of experiments (DoE) runs used to test the nanoparticle formulation variables.

Table 4. Different Factors and Their Ranges in Design-Expert Software with Constraints for Dependent Variables

factors	levels and ranges		
	−1	0	+1
sodium alginate concentration (%w/v) (A)	0.03	0.045	0.06
calcium chloride concentration (mM) (B)	18	27	36
dependent variables	constraints		
response 1 = particle size (nm) (priority set at: + ++)	336.5−592.5		
response 2 = drug content (%) (priority set at: + ++++)	7.01−14.00		

The last step of the optimization process involves the identification of a region (yellow region) in the design space, through which a robust formulation can be developed. The identified region can suggest a formulation for which dependent responses can be predicted accurately. For this, constraints and priority for dependent and independent variables were set in the software (Table 4), and an overlay plot was generated, in which a yellow region was identified (Figure 2). Further, as suggested by this region, when a formulation was prepared and evaluated for particle size and drug content, observed values were approximately equal to predicted values. Therefore, it can be ascertained that this model gives the best fit, and it is validated.

2.3. Characterization of Complex-Loaded Nanoparticles. *2.3.1. Particle Size and PDI.* The particle size and PDI of all of the formulations were calculated by the dynamic light scattering technique and are reported in Table 5. The effect of sodium alginate concentration and calcium chloride concentration was studied on particle size. It was observed that with an increase in the concentration of sodium alginate from 0.03 to 0.06% w/v, particle size increased from 336.5 to 592.5 nm, whereas particle size decreased with an increase in the concentration of calcium chloride from 18 to 36 mM, as shown in Figure 2b. This confirms that the smaller particle size is obtained when the interaction of the functional groups of sodium alginate and chitosan is in a stoichiometric proportion.[29] Further, when fitted onto the central composite design, analysis
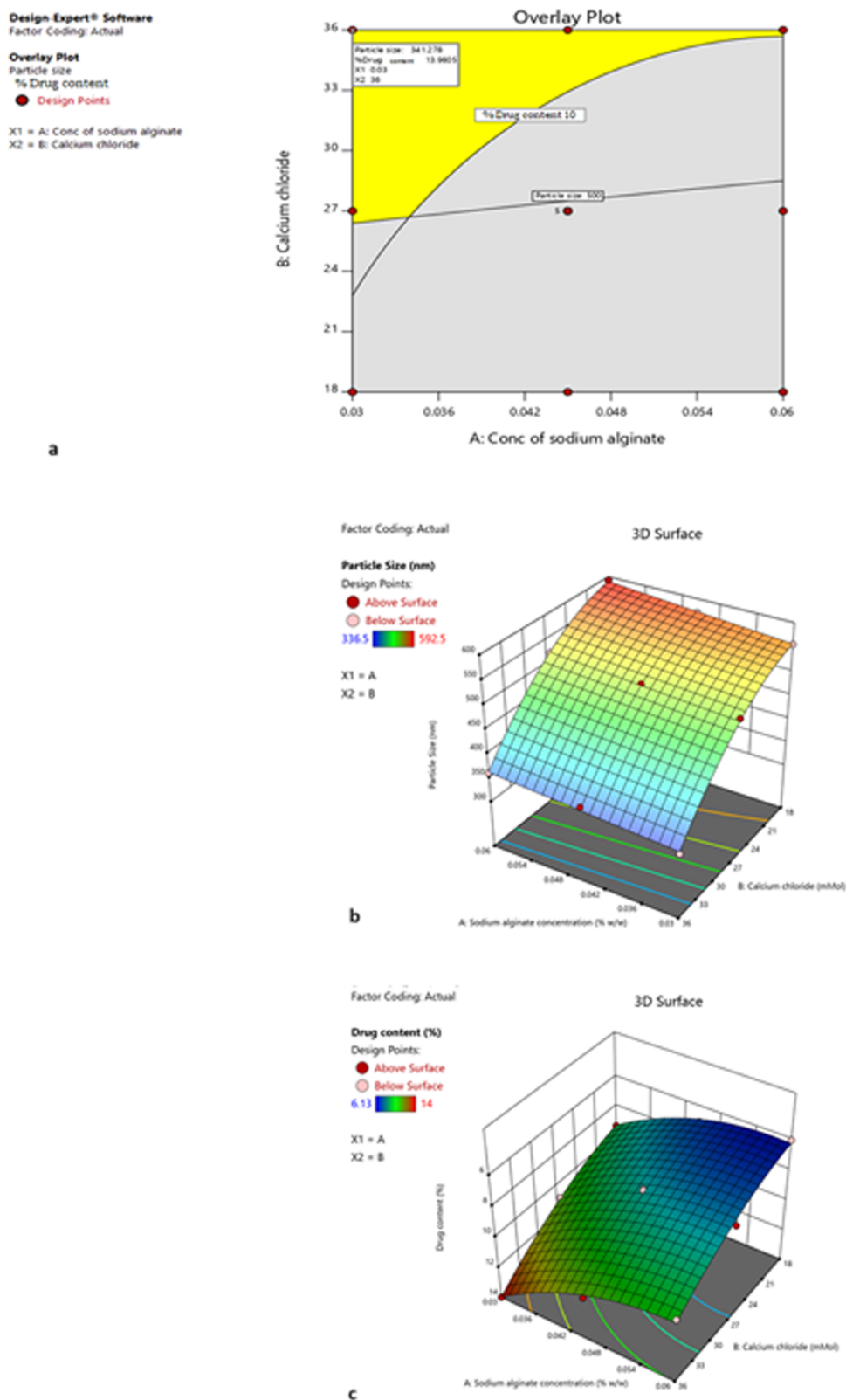
Figure 2. Overlay plot generated by Design-Expert depicting a robust yellow region (a). 3D response surface graph depicting the effect of independent variables on particle size (b) and on drug content (c).

of variance (ANOVA) suggested that the model is quadratic in nature, having an R^2 value of 0.9982 with a significant model F-value and a nonsignificant lack of fit probability (P) value of 761.77 and 3.82, respectively.

2.3.2. Drug Content and Encapsulation Efficiency. Determination of % drug content and encapsulation efficiency is important to ensure efficient drug delivery. For all of the suggested combinations, % drug content was calculated and is enlisted in Table 5. It was noted that the observed values of drug

Table 5. Formulation Runs with Dependent Variable Responses

| S. No.	formulation code	sodium alginate concentration (%w/v)	calcium chloride concentration (mM)	particle size (nm) mean ± SD ($N = 3$)	PDI mean ± SD ($N = 3$)	% drug content mean ± SD ($N = 3$)
1	F01	0.030	18	556.60 ± 2.30	0.31 ± 0.02	9.30 ± 0.68
11	F02	0.045	27	507.10 ± 1.50	0.58 ± 0.07	8.03 ± 0.79
13	F03	0.045	27	501.20 ± 1.70	0.62 ± 0.05	8.11 ± 0.53
10	F04	0.045	27	509.24 ± 0.98	0.10 ± 0.01	8.20 ± 0.54
12	F05	0.045	27	503.62 ± 3.10	0.45 ± 0.06	8.09 ± 0.94
5	F06	0.030	27	498.50 ± 2.90	0.26 ± 0.03	10.90 ± 0.12
9	F07	0.045	27	505.50 ± 1.60	0.29 ± 0.04	8.77 ± 0.32
8	F08	0.045	36	358.20 ± 0.96	0.41 ± 0.08	11.30 ± 0.65
7	F09	0.045	18	571.70 ± 3.50	0.69 ± 0.01	7.01 ± 0.15
6	F10	0.060	27	519.10 ± 3.0	0.84 ± 0.03	7.98 ± 0.19
2	F11	0.060	18	592.50 ± 1.78	0.47 ± 0.06	6.13 ± 0.21
4	F12	0.060	36	361.90 ± 1.69	0.49 ± 0.09	9.89 ± 0.24
3	F13[a]	0.030	36	0 ± 2.30	0.23 ± 0.03	14.00 ± 0.89

[a]Optimized formulation.
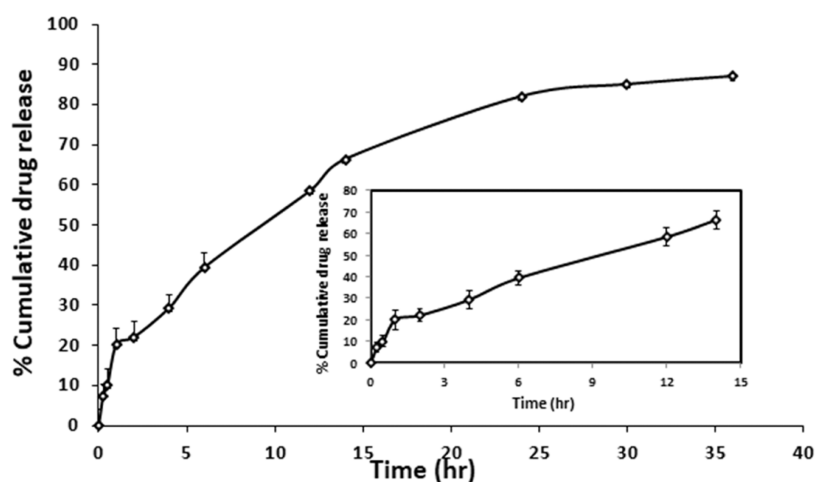
Figure 3. In vitro drug release behavior of optimized nanoparticles.

content were near the suggested values. For the optimized formulation, drug content was found to be 14 ± 0.89%, indicating that in the total weight of nanoparticles, 14% doxycycline was present. It was observed that by increasing the amount of sodium alginate from 0.03 to 0.06% w/v, drug content decreases from 14.00 to 6.13%, whereas by increasing the concentration of calcium chloride from 18 to 36 mM, drug content increases, as shown in Figure 2c. Also, there existed an inverse relation between particle size and drug content, which can be explained on the basis of the fact that at higher concentrations of sodium alginate, it is sodium alginate that forms bulk of the particle, and less volume is available for drug entrapment, thereby contributing to less drug content.[29] In this case also, when fitted into the central composite design, ANOVA suggests that the model is quadratic in nature, having an R^2 value of 0.9858 with a significant model F-value and a nonsignificant lack of fit p-value of 96.85 and 1.33, respectively. Also, as per thermogravimetric analysis (TGA), the content of HAP in nanoparticles was found to be 11.90%.

The encapsulation efficiency of the nanoparticles for doxycycline was found to be 41.77%. This indicated that around 41.77% of total doxycycline added during development was entrapped inside the particles.

2.3.3. Zeta Potential. The ζ potential is the indicator of the surface charge of nanoparticles and describes the stability of the dispersion system based on DLVO theory. As per the theory, van der Waals attractive and electrostatic repulsive forces are the determinants of system stability.[30] A high ζ potential value indicates high repulsive electrostatic forces between the particles and hence a more stable system, whereas a low value indicates high attractive forces and hence particle aggregation. The optimized placebo nanoparticle dispersion and composite-loaded nanoparticle dispersion have ζ potentials of −8.80 ± 3.8 and −13.5 ± 4.79 mV, respectively. A negative value of ζ potential is an outcome of the ionic gelation mechanism of nanoparticle preparation, through which the positive charge of the NH_3^+ groups of chitosan is neutralized by the negative charge of sodium alginate. The sodium alginate/chitosan ratio also affects the ζ potential of nanoparticles. A higher concentration of sodium alginate than that of chitosan gives rise to a high number of un-neutralized carboxylic groups due to the unavailability of the NH_3 groups of chitosan. Therefore, a high sodium alginate concentration gives rise to a negative ζ potential value.[31] Although the mucosal membrane surface charge is negative, if the nanoparticle has a positive charge, then good mucoadhesion can be obtained, but as inside the periodontal cavity, no mucoadhesion is required; henceforth, negative charge nanoparticles can also be used. Also, as per the Food and Drug Administration (FDA), nanoparticles with

negative ζ potential are less toxic to the cells than the nanoparticles with positive ζ potential.[32]

2.3.4. Drug Release. In vitro drug release from the nanoparticles in GCF 7.6 was performed through the dialysis bag method for 36 h, wherein the burst release of about 20% of the drug was observed in the initial 1 h (Figure 3). The hydrophilicity of sodium alginate contributed to the rapid hydration of nanoparticles, and further, the porous nature of particles ensured fast penetration of the dissolution medium, thereby leading to the burst release of the drug.[22] Also, the high solubility of the drug is also a major contributor to rapid release from particles.

The burst release is then followed by a slow and gradual release of about 81% of the drug for the following 25 h. This gradual release behavior can be the outcome of the swelling of sodium alginate and calcium chloride cross-linking. Due to the presence of the external phase (dissolution medium), ion exchange between Ca^{2+} and Na^+ takes place for binding with COO^-, and this leads to increased electrostatic repulsion between COO^- groups and thus chain relaxation in nanoparticles and drug release. Therefore, diffusion appears to be the main reason for this type of drug release behavior from nanoparticles.[33] When fitted into release kinetics, it followed the Higuchi model, which further confirms the diffusion mechanism (Table 6). The model that best fitted the release data was

Table 6. Regression Coefficient (R2) and Reaction Constant (K) for Different Release Kinetics Models

model	R^2	K
zero order	0.9523	0.0432
first order	0.9857	0.0307
Higuchi	0.9858	0.1745
Korsmeyer-Peppas	0.3373	0.7422
Hixon Crowell	0.8236	0.3038

selected on the basis of the regression coefficient values of various models. The Higuchi model describes the release of drugs from an insoluble matrix as a square root of the time-dependent process.[34,35] However, after 25 h, the sustained release behavior of the remaining drug was observed.

2.3.5. Particle Morphology. 2.3.5.1. Scanning Electron Microscopy (SEM). The surface morphology of adsorbed composite-loaded nanoparticles showed that particles were spherical in shape, were monodispersed in nature, and possessed a rough surface (Figure 4a). It is reported that the rough surface of the nanoparticles may help in cell adhesion and attachment at the site of action.[36]

2.3.5.2. Transmission Electron Microscopy (TEM). The TEM image of adsorbed composite-loaded nanoparticles confirmed that the agglomerate of particles did not form and was of similar size as observed via DLS (Figure 4b).

2.4. Cell Viability Assessment. *2.4.1. Murine Fibroblast (NIH3T3) Cells.* The effect of different concentrations of doxy, HAP, and nanoparticles on NIH3T3 cells was studied by the MTT (3-[4,5-dimethylthiazol-2-yl]-2,5 diphenyltetrazolium bromide) cell viability assay. It is based on the capability of live cells to reduce a yellow, water-soluble tetrazolium dye into a water-insoluble purple formazan product. Therefore, the higher the amount of formazan produced, the higher the viable cells and hence the higher the optical density of the well. Upon treatment of cells with different concentrations of doxy (10−1000 ng/mL), % cell viability decreases from 24 to 72 h. 102% cell
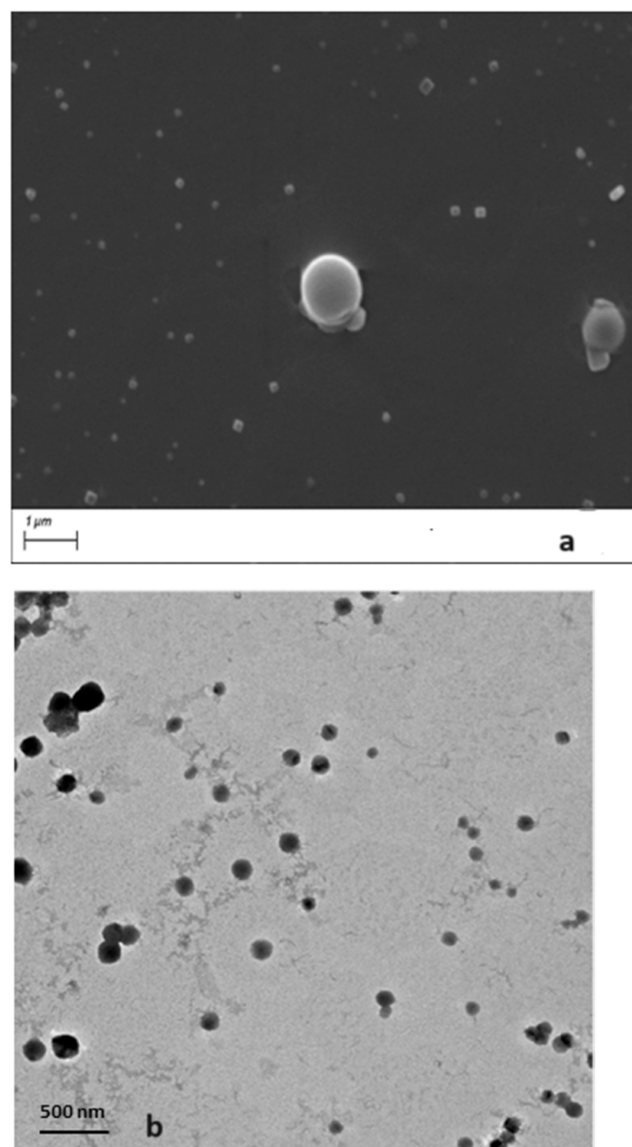

Figure 4. Scanning electron micrograph of optimized adsorbed composite-loaded nanoparticles (a) and transmission electron micrograph of optimized adsorbed composite-loaded nanoparticles (b).

viability was observed with 100 ng/mL concentration of doxy upon 24 h treatment. When treated with HAP (1−100 μg/mL), similar behavior was observed, and % cell viability decreased from 24 to 72 h. With 1 μg/mL concentration of HAP, 99.76% cell viability was observed after 24 h treatment. However, when treated with placebo and composite-loaded nanoparticles, % cell viability increased from 24 to 72 h, and 61.32 and 98.68% cells were found viable after 72 h treatment with placebo and composite-loaded nanoparticles, respectively, as shown in Figure 5. In conclusion, doxy (100 ng/mL) and HAP (1 μg/mL) support cell growth for 24 h only, whereas when combined together inside the nanoparticles, they promote cell growth until 72 h. A subsequent increase in cell viability with an increase in treatment time suggests the biocompatibility of the composite-loaded nanoparticles with the cells. Also, it has been reported that more than 70% cell viability is safe,[37] henceforth confirming the less toxic nature of composite-loaded nanoparticles. ANOVA suggests a statistically significant ($P < 0.001$) difference between all of the groups at 24, 48, and 72 h. To estimate the
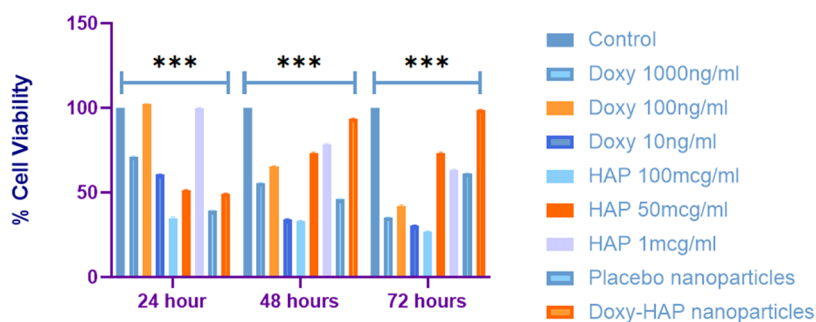
Figure 5. % Viability of NIH3T3 cells upon treatment with test substances. Data represented as mean+SD with $n = 3$ and $P < 0.001$. "***" depicts the level of significance.
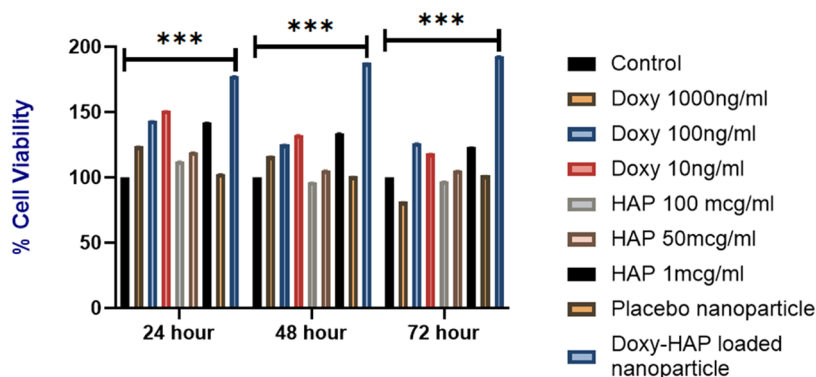

Figure 6. % Cell viability of hPDL cells upon treatment with test substances. Data represented as mean+SD with $n = 3$ and $P < 0.001$. "***" depicts the level of significance.

statistical difference between different groups and the control group at all time intervals, Bonferroni post hoc multiple analysis was performed.

2.4.2. Human Periodontal Ligament Cells (hPDLC). The effect of different concentrations of doxy, HAP, placebo, and composite-loaded nanoparticles on hPDL cells was studied by the MTT cell viability assay. Upon treatment of cells with different concentrations of doxy (10−1000 ng/mL), % cell viability decreases from 24 to 72 h. 151% cell viability was observed with a 10 ng/mL concentration of doxy after 24 h treatment. As cells were found to proliferate, instead of cell viability, the cell proliferation term was used to measure cell growth. When treated with HAP (1−100 μg/mL), similar behavior was observed, and the % cell proliferation decreased from 24 to 72 h. With 1 μg/mL concentration of HAP, 141.8% cell proliferation was observed after 24 h treatment. When treated with placebo nanoparticles, % cell proliferation equivalent to control was noted, which is more than 70%, thereby indicating the biocompatible nature[37] of sodium alginate and chitosan. However, when treated with composite-loaded nanoparticles, cell proliferation increases from 177.86 to 192.98% in 72 h, as shown in Figure 6. Similar to NIH3T3 cells, increased hPDL cell viability was also observed with composite-loaded nanoparticles as compared to doxy and HAP alone in due course of time. ANOVA suggests a statistically significant ($P < 0.001$) difference between all of the groups at time periods of 24, 48, and 72 h.

2.4.3. Stability Studies. To assess the stability of lyophilized nanoparticles during storage, particle size, PDI, and % drug content were determined at intervals of 0, 1, 2, 3, and 4 weeks, and it was found that results did not vary considerably and remained in the desired limit, as shown in Table 7.

Table 7. Time-Dependent Responses of the Optimized Formulation during the Stability Study

weeks	particle size mean ± SD ($N = 3$)	PDI mean ± SD ($N = 3$)	% drug content mean ± SD ($N = 3$)
0	340 ± 0.34	0.29 ± 0.05	13.9 ± 0.39
1	346 ± 0.78	0.32 ± 0.09	13.2 ± 0. 36
2	350 ± 0.91	0.39 ± 0.06	12.7 ± 0.89
3	357 ± 0.38	0.46 ± 0.02	12.5 ± 0.74
4	369 ± 0.67	0.49 ± 0.03	11.9 ± 0.82

3. CONCLUSIONS

Sodium alginate−chitosan nanoparticles containing an adsorbed composite of doxy and HAP were successfully fabricated by the ionic gelation method with quality by design approaches. The initial risk assessment was performed and optimized by Design-Expert software, and a design space was generated on which a robust or optimized formulation could be obtained. A particle size of 336.5 nm, a PDI of 0.23, a ζ potential of −13.5 mV, and surface morphology via SEM and TEM confirmed the good size, shape, and rough nature of nanoparticles. Although 14% drug content, 11.90% HAP content, and 41.77% drug encapsulation efficiency of the nanoparticles are less, they were capable of carrying enough doxy and HAP. The in vitro study confirms the sustained release behavior of doxy from the nanoparticles up to 36 h. The in vitro % viability study conducted on NIH3T3 cells depicts the lesser cytoprotective nature of the formulation as compared to doxy and HAP alone. Nonetheless, in the case of hPDL cells, significant viability was observed, which indicated that the formulation supported the growth of human cells. Further, the stability study ensures the stable nature of nanoparticles for 4 weeks in terms of size, PDI,

and drug content. In summary, sodium alginate–chitosan nanoparticles may be used as a suitable carrier for the codelivery of doxy and HAP for periodontal therapy and further need to be subjected to preclinical and clinical evaluation.

4. MATERIALS AND METHODS

4.1. Materials. Sodium alginate (medium viscosity), calcium chloride, and chitosan (medium viscosity) were obtained as gift samples from Jubilant Life Sciences, Noida, India. Doxycycline hyclate was obtained ex gratia from Sun Pharma, India, and hydroxyapatite was purchased from Sigma-Aldrich, India. The NIH3T3 cell line was purchased from the National Center for Cell Science (NCCS), Pune. Dulbecco's minimal Eagle medium (DMEM), fetal bovine serum (FBS), and trypsin phosphate versene glucose (TPVG) were purchased from Thermo Fisher Scientific, India. All other chemicals were of analytical grade.

4.2. Methods. *4.2.1. Development and Characterization of HAP-Doxy-Adsorbed Composite.* The physical adsorption method was adopted to develop the composite of doxycycline hyclate and HAP. Doxy and HAP (3:1) were suspended in distilled water, and the suspension was allowed to evaporate under constant stirring at 200 ± 5 rpm for 24 h at 45 °C. After complete drying, the adsorbed composite was stored in a cool and dry place. The developed complex was characterized on the basis of surface morphology by SEM, so as to confirm the development of the complex.[38]

Further, in order to calculate the amount of drug adhered to the HAP surface, a weighed amount of the HAP-Doxy dried composite was added to 10 mL of water. The suspension was then filtered with the help of Whatman filter paper, and the unadsorbed drug in solution was determined with a UV–visible spectrophotometer (UV-1601, Shimadzu, Japan) at 271.5 nm.

4.2.2. Development and Optimization of HAP-Doxy-Adsorbed Composite-Loaded Nanoparticles. Nanoparticles were prepared by a cation-induced controlled gelification method. A 0.03–0.06%w/v aqueous solution of sodium alginate was prepared, and 1 mL of an 18–36 mM calcium chloride solution was added dropwise with stirring at 1200 ± 50 rpm for 3 h at room temperature.[39] This resulted in the formation of the pregel phase.

A 0.03% w/v aqueous solution of chitosan was prepared in acetic acid (1.5%v/v pH 2.3) and then neutralized to pH 4.6 with sodium hydroxide solution. Then, the neutralized chitosan solution was added dropwise into the pregel phase (alginate/chitosan ratio maintained as 10:1) at 1200 ± 50 rpm and stirred overnight for a uniform coating at room temperature.[40] The resulting dispersion was centrifuged at 14,000 rpm to separate the nanoparticles. The obtained nanoparticle pallet was washed, redispersed, and lyophilized to collect the dried form.

In order to prepare the adsorbed composite-loaded nanoparticles, a weighed amount of the composite was added to the sodium alginate solution (with composite/polymer w/w ratio of 1:1), and then the above-mentioned procedure was followed.

Optimization was done using the quality by design (QbD) approach, which includes three major steps—initial risk assessment, design of experimentation (DoE), and, finally, model validation.[25] For the initial risk assessment, sodium alginate and calcium chloride concentrations, speed of rotation, time of stirring, chitosan concentration, and amount of the composite were evaluated, and their effects on particle size and uniformity were studied by conducting different formulation trials. The quality target product profile (QTPP) of the final product was established as per the literature, and based on this,

the particle size and % drug content of the nanoparticles were selected as dependent factors. From the initial risk assessment, it was found that two independent factors, namely, concentrations of sodium alginate (%w/v) and calcium chloride (mM), were the critical parameters that could affect the critical quality attributes of nanoparticles. With the help of central composite design (CCD), 13 combinations of independent factors were formulated, and their effect on dependent variables was noted and fed into Design-Expert 11 by Stat-Ease software to develop a design model or design space that can accurately predict an optimized formulation. A composition suggested by CCD was taken as the optimized formula for nanoparticle development.

4.2.3. Characterization of Adsorbed Composite-Loaded Nanoparticles. 4.2.3.1. Particle Size and PDI. For the stability and homogeneity of nanoparticles, the average particle size and polydispersity index are the important parameters. Therefore, particle size and PDI were determined by a Malvern Zetasizer (Malvern Instruments, UK) based on the dynamic light scattering technique (DLS) by 10 times diluting 100 μL of the nanoparticle sample with deionized water. Each sample was assessed in triplicate.[41]

4.2.3.2. Drug Content and Encapsulation Efficiency. To determine the drug content, a weighed amount of lyophilized nanoparticles was added to 10 mL of distilled water and kept at 200 ± 5 rpm in a shaker incubator for 24 h to ensure the complete release of doxy and HAP from nanoparticles. The supernatant was then filtered through a 0.45 μm filter and injected in a reverse-phase high-performance liquid chromatography (RP-HPLC) system (Water e2695) to determine the doxy concentration. Further, drug content and encapsulation efficiency were calculated with eqs 1 and 2, respectively.[42]

$$\% \text{ drug content} = (W_S/W_N) \times 100 \tag{1}$$

where W_S is the amount of the drug in the sample and W_N is the amount of the lyophilized sample taken.

$$\% \text{ encapsulation efficiency} = (W_S/W_T) \times 100 \tag{2}$$

where W_S is the amount of the drug in the sample and W_T is the amount of the drug initially added to the nanoparticles.

In order to determine the content of HAP in the nanoparticles, thermogravimetric analysis (TGA) was carried out on a thermal analyzer (Mettler Toledo AG Analytical, CH-8603, Schwerzenbach). The technique determines the rate of change of the weight of the subjected material as a function of temperature. Nanoparticles were weighed and placed in silica crucibles and subjected to a heating tunnel at a temperature range of 30–700 °C with a nitrogen flow rate of 20 mL/min at a scanning rate of 10 °C/min.[43] After complete heating, the remaining weight of the sample indicated the amount of HAP in the sample.

4.2.3.3. Zeta Potential. Determination of the ζ potential is important to ensure the stability of nanoparticles. Therefore, diluted samples of nanoparticles, i.e., placebo and composite-loaded nanoparticles in deionized water (100 times dilution), were subjected for ζ potential determination in a Malvern Zetasizer (Malvern Instruments, UK) in triplicate.[42]

4.2.3.4. Drug Release. In vitro drug release from nanoparticles was carried out for 36 h in simulated GCF pH 7.6 using the dialysis bag (D9777, Dialysis tubing cellulose membrane, 14 kDa mol. Wt., Sigma-Aldrich) method. A weighed quantity of lyophilized nanoparticles was suspended separately in 1.5 mL of simulated GCF and was then filled in an activated dialysis bag,

which was then suspended in a beaker containing 100 mL of simulated GCF and kept in an incubator shaker at $35 \pm 0.5\ °C$ and 100 ± 5 rpm for 36 h. 5 mL of samples were withdrawn at appropriate time intervals and replaced with fresh dissolution media, i.e., GCF, to maintain the sink condition. All the samples (collected in triplicate) were filtered through a 0.45 μm syringe filter and analyzed through RP-HPLC. The results were reported as the mean $\pm$ SD of three replicates ($N = 3$).[38] Further, the obtained data were analyzed, and the release kinetics for the drugs was determined.

4.2.3.5. Particle Morphology. Scanning electron microscopy (SEM): To study the surface morphology of nanoparticles, samples were placed in a silver paint-coated aluminum stub and dried. Then, the sample was sputter-coated by a gold layer and observed under a scanning electron microscope (EVO 18, Zeiss, Germany).[44]

Transmission electron microscopy (TEM): TEM of nanoparticles was performed after negative staining with phosphotungstic acid (PTA). A drop of dispersion (1 mg/mL) was placed on copper grids, and then, a drop of PTA was added to this. Later on, excess liquid was removed, and the grid was air-dried and subjected to imaging under a transmission electron microscope.[45]

4.2.4. Cell Viability Assessment. 4.2.4.1. Murine Fibroblast (NIH3T3) Cells. In order to assess the viability, murine NIH3T3 cells after 3−4 passaging were incubated at $37 \pm 2\ °C$ in a humidified atmosphere containing 95% air and 5% CO_2 in an incubator at a concentration of 15×10^3 in 200 μL of media containing DMEM (Dulbecco's minimal Eagle medium), FBS, pen−strep (10:2:1), and sodium bicarbonate in a 96-well plate for 24 h. When the cells adhered to the well plate, wells were treated at different concentrations of doxy (1000, 100, and 10 ng/mL), HAP (100, 50, and 1 μg/mL), placebo nanoparticles, and drug-loaded nanoparticles for 24, 48, and 72 h. At different time points, each well was washed with phosphate-buffered saline 7.4 (PBS), then treated with 200 μL of MTT (3-(4,5-dimethylthiazol-2-yl)-2,5-diphenyltetrazolium bromide) and PBS 7.4 (19:3 ratio), and left for 3 h for the development of formazan crystals. After 3 h, the crystals were dissolved in 200 μL of DMSO (dimethyl sulfoxide), and the optical density (OD) of each well was noted at 570 nm with the help of an ELISA plate reader (Thermo Fisher Scientific). Each experiment was performed in triplicate.[46] Further, cell viability was calculated by the following formula.

$$\% \text{ cell viability} = (\text{mean OD of treatment well} / \text{mean OD of control well}) \times 100$$

4.2.4.2. Human Periodontal Ligament Cells (hPDLC). The experiments were performed in accordance with the guidelines for medical ethics and research of the Jamia Hamdard. The study design and experiments were approved by the Ethics Committee of Jamia Hamdard. All participants were provided written informed consent to participate in this study.

Six healthy human premolar teeth, which were extracted for orthodontic reasons, were collected immediately in a container containing phosphate-buffered saline (PBS) with 1% antibiotic antimycotic (Gibco, Thermo Fisher Scientific). The extracted teeth were then washed 4−5 times using phosphate buffer in a sterile Petri dish in a biosafety cabinet. The middle-third of the roots were scraped gently using a surgical blade into a sterile Petri dish. The obtained tissues were then minced into smaller pieces and digested with freshly prepared 3 mg/mL collagenase

type I solution (Gibco, Thermo Fisher Scientific) with incubation at $37 \pm 2\ °C$ in 5% CO_2 for 45 min. Next to this, an equal amount of DMEM was added to neutralize the action of the enzyme.[47] The mixture was then transferred to a T25 flask containing complete culture media (88% Dulbecco's modified Eagle medium (Gibco), 10% fetal bovine serum (Gibco), and 1% penicillin−streptomycin (Gibco). The flask was placed in a humidified atmosphere of $37\ °C$ and 5% CO_2 for 3 days. The medium was changed every third day. Floating cells were removed after 3 days, and the adherent cells were further expanded and cryopreserved in liquid nitrogen for subsequent use. Experiments were performed using either passage 4 or 5 cells.[48] In order to assess the cell viability, a similar procedure as explained in Section 4.2.4.1 was performed, and % cell viability was calculated.

4.3. Statistical Analysis. Statistical analysis was carried out using GraphPad Prism 8.4.2 (GraphPad Software, San Diego, CA) and Microsoft Excel 2021. The ANOVA test and then the Bonferroni post hoc test for multiple comparisons were used for statistical analysis between groups.

Quantitative variables were expressed as mean values $\pm$ standard deviation. A p-value ≤ 0.05 indicated statistical significance.

■ AUTHOR INFORMATION

Corresponding Author

Zeenat Iqbal − *Department of Pharmaceutics, School of Pharmaceutical Education and Research, SPER, Jamia Hamdard, New Delhi 110062, India;* orcid.org/0000-0003-2788-9420; Phone: 011-26058689-5662; Email: zeenatiqbal@jamiahamdard.ac.in; Fax: 011-26059663

Authors

Pooja Jain − *Department of Pharmaceutics, School of Pharmaceutical Education and Research, SPER, Jamia Hamdard, New Delhi 110062, India*

Mohd. Aamir Mirza − *Department of Pharmaceutics, School of Pharmaceutical Education and Research, SPER, Jamia Hamdard, New Delhi 110062, India;* orcid.org/0000-0002-5780-7601

Enam Reyaz − *Department of Molecular Medicine, Jamia Hamdard, New Delhi 110062, India*

Mirza Adil Beg − *Department of Molecular Medicine, Jamia Hamdard, New Delhi 110062, India*

Angamuthu Selvapandiyan − *Department of Molecular Medicine, Jamia Hamdard, New Delhi 110062, India;* orcid.org/0000-0002-2194-1534

Nazeer Hasan − *Department of Pharmaceutics, School of Pharmaceutical Education and Research, SPER, Jamia Hamdard, New Delhi 110062, India*

Akbar Naqvi − *Department of Dentistry, HIMSR, New Delhi 110062, India*

Naseef Punnoth Poonkuzhi − *Department of Pharmaceutics, Moulana College of Pharmacy, Perinthalmanna, Kerala 679321, India;* orcid.org/0000-0001-9692-6323

Mohammad Saheer Kuruniyan − *Department of Dental Technology, COAMS, King Khalid University, Abha 61421, Saudi Arabia*

Harlokesh Narayan Yadav − *Department of Pharmacology, AIIMS, New Delhi 110608, India*

Farhan J. Ahmad − *Department of Pharmaceutics, School of Pharmaceutical Education and Research, SPER, Jamia*

Hamdard, New Delhi 110062, India; ◉ orcid.org/0000-0002-0740-8573

Complete contact information is available at:
https://pubs.acs.org/10.1021/acsomega.3c07092

Author Contributions

P.J.: data curation, investigation, writing—original draft, and writing—review and editing. M.A.M.: visualization and writing—review and editing. E.R., M.A.B., and N.H.: data curation. A.S.: formal analysis. Dr. A.N.: methodology. N.P.P. and M.S.K.: funding acquisition. H.N.Y., F.J.A., and Z.I.: supervision.

Notes

The authors declare no competing financial interest.

■ ACKNOWLEDGMENTS

■ SYMBOLS AND NOTATIONS

MMP	matrix metalloproteinase
PDI	polydispersity index
mV	millivolt
SEM	scanning electron microscopy
TEM	transmission electron microscopy
GCF	gingival crevicular fluid
NIH3T3	murine fibroblast cells
hPDL	human periodontal ligament
Doxy	doxycycline hyclate
HAP	hydroxyapatite
QbD	quality by design
QTPP	quality target product profile
CQA	critical quality attributes
nm	nanometer
SA	sodium alginate
mM	millimolar
mg	milligram
w/v	weight/volume
w/w	weight/weight
DoE	design of experiments
rpm	rotation per minute
R^2	coefficient of regression
ANOVA	analysis of variance
P	probability
N	number of runs
SD	standard deviation
TGA	thermogravimetric analysis
K	reaction constant
DLS	dynamic light scattering
DMEM	Dulbecco's minimal Eagle medium
FBS	fetal bovine serum
TPVG	trypsin phosphate versene glucose
CCD	central composite design
RP-HPLC	reverse-phase high-performance liquid chromatography
W_S	amount of the drug in the sample

W_N	amount of the lyophilized sample taken
W_T	amount of the drug initially added to the nanoparticles
mL	milliliter
μm	micrometer
μL	microliter
PTA	phosphotungstic acid

■ REFERENCES

(1) Jain, P.; Mirza, M. A.; Iqbal, Z. A 4-D Approach for Amelioration of Periodontitis. *Med. Hypotheses* **2019**, *133*, No. 109392.

(2) Jain, P.; Hassan, N.; Khatoon, K.; Mirza, M.; Naseef, P. P.; Kuruniyan, M. S.; Iqbal, Z. Periodontitis and Systemic Disorder—An Overview of Relation and Novel Treatment Modalities. *Pharmaceutics* **2021**, *13* (8), 1175.

(3) Iqbal, D. Z.; Mirza, M. A.; Iqbal, Z. Unraveling the Etiology of Periodontitis. *Int. J. Biomed. Invest.* **2021**, *4* (1), 1−4.

(4) Gupta, S.; Mohindra, R.; Singla, M.; Khera, S.; Sahni, V.; Kanta, P.; Soni, R. K.; Kumar, A.; Gauba, K.; Goyal, K.; et al. The Clinical Association between Periodontitis and COVID-19. *Clin. Oral Invest.* **2021**, *26*, 1361−1374, DOI: 10.1007/s00784-021-04111-3.

(5) Fabri, G. M. C. Potential Link between COVID-19 and Periodontitis: Cytokine Storm, Immunosuppression, and Dysbiosis. *Oral Health and Dental Management* **2020**, *20* (1), 1−5.

(6) Wei, Y.; Deng, Y.; Ma, S.; Ran, M.; Jia, Y.; Meng, J.; Han, F.; Gou, J.; Yin, T.; He, H.; et al. Local Drug Delivery Systems as Therapeutic Strategies against Periodontitis: A Systematic Review. *J. Controlled Release* **2021**, *333*, 269−282.

(7) Isola, G.; Polizzi, A.; Santonocito, S.; Dalessandri, D.; Migliorati, M.; Indelicato, F. New Frontiers on Adjuvants Drug Strategies and Treatments in Periodontitis. *Sci. Pharm.* **2021**, *89* (4), No. 46.

(8) Graziani, F.; Karapetsa, D.; Alonso, B.; Herrera, D. Nonsurgical and Surgical Treatment of Periodontitis: How Many Options for One Disease? *Periodontology 2000* **2017**, *75* (1), 152−188.

(9) Ogut, D.; Reel, B.; Korkmaz, C. G.; Arun, M. Z.; Micili, S. C.; Ergur, B. U. Doxycycline Down-Regulates Matrix Metalloproteinase Expression and Inhibits NF-KB Signaling in LPS-Induced PC3 Cells. *Folia Histochem. Cytobiol.* **2016**, *54* (4), 171−180.

(10) Sundararaj, S. C.; Thomas, M. V.; Peyyala, R.; Dziubla, T. D.; Puleo, D. A. Design of a Multiple Drug Delivery System Directed at Periodontitis. *Biomaterials* **2013**, *34* (34), 8835−8842.

(11) Jain, P.; Aamir Mirza, M.; Talegaonkar, S.; Nandy, S.; Dudeja, M.; Sharma, N.; Khalid Anwer, M.; M Alshahrani, S.; Iqbal, Z. Design and in Vitro/in Vivo Evaluations of a Multiple-Drug-Containing Gingiva Disc for Periodontotherapy. *RSC Adv.* **2020**, *10* (14), 8530−8538.

(12) Jain, P.; Farooq, U.; Nainwal, L. M.; Alam, M.; Kuruniyan, M. S.; Mirza, M. A.; Iqbal, Z. In-Silico Validation of the Proposed Treatment Strategy of Periodontitis. *Comb. Chem. High Throughput Screening* **2022**, *25*, 2295−2313, DOI: 10.2174/1386207325666220126102235.

(13) Jain, P.; Farooq, U.; Hassan, N.; Albratty, M.; Alam, M. S.; Makeen, H. A.; Mirza, M. A.; Iqbal, Z. Nanotechnology Interventions as a Putative Tool for the Treatment of Dental Afflictions. *Nanotechnol. Rev.* **2022**, *11* (1), 1935−1946.

(14) Jain, P.; Dilnawaz, F.; Iqbal, Z. Insights into Nanotools for Dental Interventions. In *Nanopharmaceuticals: Principles and Applications Vol. 3*; Yata, V. K.; Ranjan, S.; Dasgupta, N.; Lichtfouse, E., Eds.; Springer International Publishing: Cham, 2020; pp 53−79 DOI: 10.1007/978-3-030-47120-0_3.

(15) Szulc, M.; Zakrzewska, A.; Zborowsk, J. Local Drug Delivery in Periodontitis Treatment: A Review of Contemporary Literature. *Dent Med. Probl* **2018**, *55* (3), 333−342.

(16) Rajeshwari, H. R.; Dhamecha, D.; Jagwani, S.; Rao, M.; Jadhav, K.; Shaikh, S.; Puzhankara, L.; Jalalpure, S. Local Drug Delivery Systems in the Management of Periodontitis: A Scientific Review. *J. Controlled Release* **2019**, *307*, 393−409.

(17) Li, Q.; Zhou, Y.; He, W.; Ren, X.; Zhang, M.; Jiang, Y.; Zhou, Z.; Luan, Y. Platelet-Armored Nanoplatform to Harmonize Janus-Faced

IFN-γ against Tumor Recurrence and Metastasis. *J. Controlled Release* **2021**, *338*, 33−45.

(18) Vinothini, K.; Dhilip Kumar, S. S.; Abrahamse, H.; Rajan, M. Enhanced Doxorubicin Delivery in Folate-Overexpressed Breast Cancer Cells Using Mesoporous Carbon Nanospheres. *ACS Omega* **2021**, *6* (50), 34532−34545.

(19) Ding, L.; Zhang, P.; Wang, X.; Kasugai, S. A Doxycycline-Treated Hydroxyapatite Implant Surface Attenuates the Progression of Peri-Implantitis: A Radiographic and Histological Study in Mice. *Clin. Implant Dent. Relat. Res.* **2019**, *21* (1), 154−159.

(20) Andrei, V.; Andrei, S.; Gal, A. F.; Rus, V.; Gherman, L.-M.; Boşca, B. A.; Niculae, M.; Barabas, R.; Cadar, O.; Dinte, E.; Muntean, D.-M.; Peştean, C. P.; Rotar, H.; Boca, A.; Chiş, A.; Tăut, M.; Candrea, S.; Ilea, A. Immunomodulatory Effect of Novel Electrospun Nanofibers Loaded with Doxycycline as an Adjuvant Treatment in Periodontitis. *Pharmaceutics* **2023**, *15* (2), 707.

(21) Semyari, H.; Salehi, M.; Taleghani, F.; Ehterami, A.; Bastami, F.; Jalayer, T.; Semyari, H.; Hamed Nabavi, M.; Semyari, H. Fabrication and Characterization of Collagen−Hydroxyapatite-Based Composite Scaffolds Containing Doxycycline via Freeze-Casting Method for Bone Tissue Engineering. *J. Biomater. Appl.* **2018**, *33* (4), 501−513.

(22) Ji, M.; Sun, X.; Guo, X.; Zhu, W.; Wu, J.; Chen, L.; Wang, J.; Chen, M.; Cheng, C.; Zhang, Q. Green Synthesis, Characterization and in Vitro Release of Cinnamaldehyde/Sodium Alginate/Chitosan Nanoparticles. *Food Hydrocolloids* **2019**, *90*, 515−522.

(23) Bi, Y.-g.; Lin, Z.; Deng, S. Fabrication and Characterization of Hydroxyapatite/Sodium Alginate/Chitosan Composite Microspheres for Drug Delivery and Bone Tissue Engineering. *Mater. Sci. Eng., C* **2019**, *100*, 576−583.

(24) Sah, A. K.; Dewangan, M.; Suresh, P. K. Potential of Chitosan-Based Carrier for Periodontal Drug Delivery. *Colloids Surf., B* **2019**, *178*, 185−198.

(25) Saha, M.; Saha, D. R.; Ulhosna, T.; Sharker, S. M.; Shohag, M. H.; Islam, M. S.; Ray, S. K.; Rahman, G. S.; Reza, H. M. QbD Based Development of Resveratrol-Loaded Mucoadhesive Lecithin/Chitosan Nanoparticles for Prolonged Ocular Drug Delivery. *J. Drug Delivery Sci. Technol.* **2021**, *63*, No. 102480.

(26) Adena, S. K. R.; Upadhyay, M.; Vardhan, H.; Mishra, B. Gold Nanoparticles for Sustained Antileukemia Drug Release: Development, Optimization and Evaluation by Quality-by-Design Approach. *Nanomedicine* **2019**, *14* (7), 851.

(27) Beg, S.; Dhiman, S.; Sharma, T.; Jain, A.; Sharma, R. K.; Jain, A.; Singh, B. Stimuli Responsive In Situ Gelling Systems Loaded with PLGA Nanoparticles of Moxifloxacin Hydrochloride for Effective Treatment of Periodontitis. *AAPS PharmSciTech* **2020**, *21* (3), No. 76.

(28) Jain, S. Quality by Design (QBD): A Comprehensive Understanding of Implementation and Challenges in Pharmaceuticals Development. *Int. J. Pharm. Pharm. Sci.* **2014**, *6*, 29−35.

(29) Motwani, S. K.; Chopra, S.; Talegaonkar, S.; Kohli, K.; Ahmad, F. J.; Khar, R. K. Chitosan−Sodium Alginate Nanoparticles as Submicroscopic Reservoirs for Ocular Delivery: Formulation, Optimisation and in Vitro Characterisation. *Eur. J. Pharm. Biopharm.* **2007**, *68* (3), 513−525.

(30) van Oss, C. J. The Extended DLVO Theory. In *Interface Science and Technology*; Elsevier, 2008; Vol. *16*, pp 31−48.

(31) Ahdyani, R.; Novitasari, L.; Martien, R.; Danarti, R. Formulation and Characterization of Timolol Maleate-Loaded Nanoparticles Gel by Ionic Gelation Method Using Chitosan and Sodium Alginate. *Int. J. Appl. Pharm.* **2019**, *11*, 48−54.

(32) Honary, S.; Zahir, F. Effect of Zeta Potential on the Properties of Nano-Drug Delivery Systems-a Review (Part 2). *Trop. J. Pharm. Res.* **2013**, *12* (2), 265−273.

(33) Bensouiki, S.; Belaib, F.; Sindt, M.; Magri, P.; Rup-Jacques, S.; Bensouici, C.; Meniai, A.-H. Evaluation of Anti-Inflammatory Activity and In Vitro Drug Release of Ibuprofen-Loaded Nanoparticles Based on Sodium Alginate and Chitosan. *Arab J. Sci. Eng.* **2020**, *45* (9), 7599−7609.

(34) Manuja, A.; Kumar, S.; Dilbaghi, N.; Bhanjana, G.; Chopra, M.; Kaur, H.; Kumar, R.; Manuja, B. K.; Singh, S. K.; Yadav, S. C. Quinapyramine Sulfate-Loaded Sodium Alginate Nanoparticles Show Enhanced Trypanocidal Activity. *Nanomedicine* **2014**, *9* (11), 1625−1634.

(35) Dash, S.; Murthy, P. N.; Nath, L.; Chowdhury, P. Kinetic modeling on drug release from controlled drug delivery systems. *Acta Pol. Pharm.* 67, 217 223.

(36) Cai, S.; Wu, C.; Yang, W.; Liang, W.; Yu, H.; Liu, L. Recent Advance in Surface Modification for Regulating Cell Adhesion and Behaviors. *Nanotechnol. Rev.* **2020**, *9* (1), 971−989.

(37) Barot, T.; Rawtani, D.; Kulkarni, P. Physicochemical and Biological Assessment of Silver Nanoparticles Immobilized Halloysite Nanotubes-Based Resin Composite for Dental Applications. *Heliyon* **2020**, *6* (3), No. e03601.

(38) Jain, P.; Garg, A.; Farooq, U.; Panda, A. K.; Mirza, M. A.; Noureldeen, A.; Darwish, H.; Iqbal, Z. Preparation and Quality by Design Assisted (Qb-d) Optimization of Bioceramic Loaded Microspheres for Periodontal Delivery of Doxycycline Hyclate. *Saudi J. Biol. Sci.* **2021**, *28* (5), 2677−2685.

(39) Rajaonarivony, M.; Vauthier, C.; Couarraze, G.; Puisieux, F.; Couvreur, P. Development of a New Drug Carrier Made from Alginate. *J. Pharm. Sci.* **1993**, *82* (9), 912−917.

(40) Sarmento, B.; Ribeiro, A. J.; Veiga, F.; Ferreira, D. C.; Neufeld, R. J. Insulin-Loaded Nanoparticles Are Prepared by Alginate Ionotropic Pre-Gelation Followed by Chitosan Polyelectrolyte Complexation. *J. Nanosci. Nanotechnol.* **2007**, *7* (8), 2833−2841.

(41) Jain, P.; Taleuzzaman, M.; Kala, C.; Kumar Gupta, D.; Ali, A.; Aslam, M. Quality by Design (Qbd) Assisted Development of Phytosomal Gel of Aloe Vera Extract for Topical Delivery. *J. Liposome Res.* **2020**, *31*, 381−388, DOI: 10.1080/08982104.2020.1849279.

(42) Siddiqui, L.; Bag, J.; Mittal, D.; Leekha, A.; Mishra, H.; Mishra, M.; Verma, A. K.; Mishra, P. K.; Ekielski, A.; Iqbal, Z.; et al. Assessing the Potential of Lignin Nanoparticles as Drug Carrier: Synthesis, Cytotoxicity and Genotoxicity Studies. *Int. J. Biol. Macromol.* **2020**, *152*, 786−802, DOI: 10.1016/j.ijbiomac.2020.02.311.

(43) Mishra, V. K.; Srivastava, S. K.; Asthana, B. P.; Kumar, D. Structural and Spectroscopic Studies of Hydroxyapatite Nanorods Formed via Microwave-Assisted Synthesis Route. *J. Am. Ceram. Soc.* **2012**, *95* (9), 2709−2715.

(44) Anjum, F.; Zakir, F.; Verma, D.; Aqil, M.; Singh, M.; Jain, P.; Mirza, M. A.; Anwer, Md. K.; Iqbal, Z. Exploration of Nanoethosomal Transgel of Naproxen Sodium for the Treatment of Arthritis. *Curr. Drug Delivery* **2020**, *17* (10), 885−897.

(45) Gajra, B.; Dalwadi, C.; Patel, R. Formulation and Optimization of Itraconazole Polymeric Lipid Hybrid Nanoparticles (Lipomer) Using Box Behnken Design. *DARU J. Pharm. Sci.* **2015**, *23* (1), 3.

(46) Theiszova, M.; Jantova, S.; Dragunova, J.; Grznarova, P.; Palou, M. Comparison the Cytotoxicity of Hydroxiapatite Measured by Direct Cell Counting and MTT Test in Murine Fibroblast NIH-3T3 Cells. *Biomed. Papers* **2005**, *149* (2), 393−396.

(47) Fujioka-Kobayashi, M.; Müller, H.-D.; Mueller, A.; Lussi, A.; Sculean, A.; Schmidlin, P. R.; Miron, R. J. In Vitro Effects of Hyaluronic Acid on Human Periodontal Ligament Cells. *BMC Oral Health* **2017**, *17*, 44.

(48) Banavar, S. R.; Rawal, S. Y.; Paterson, I. C.; Singh, G.; Davamani, F.; Khoo, S. P.; Tan, E. L. Establishing a Technique for Isolation and Characterization of Human Periodontal Ligament Derived Mesenchymal Stem Cells. *Saudi Dent. J.* **2021**, *33* (7), 693−701.